

Control of Grid- Interfacing Inverters with Integrated Voltage Unbalance Correction

Mohan.A, D.Nagaraju

Abstract: The control of a grid interfacing inverter with integrated voltage unbalance correction. It is proposed to add an additional function to the inverter to decrease the negative-sequence voltage at the point of connection with the utility grid. Based on symmetric sequence voltage decomposition and using an improved multi-variable filter, the grid-interfacing inverter intentionally absorbs a small amount of negative-sequence current from the grid, thereby helping to correct the negative-sequence voltage. Although the amplitude reduction contributed by each individual inverter system is small compared to the total negative-sequence component, grid interfacing inverter modules can collectively achieve substantial results in the grid. The integrated function and proposed control has been verified in simulations and by experiments on a laboratory prototype.

I. Introduction:

The voltage unbalance correction function is added, which intentionally regulates negative sequence currents. Note that, in order to obtain a maximum power factor, most grid-interfacing inverters deliver only positive-sequence currents under either balanced or unbalanced conditions. Therefore, the development of this proposed controller differs from the conventional one, and its design will be presented in the next sections of this paper.

In view of unbalanced with the theory of symmetric decomposition for three phase systems, unbalanced grid voltages can be divided into three groups, namely positive, negative, and zero sequence voltages. Similarly, current quantities can also be separated. By disregarding the mutual coupling between the grid lines in an equivalent circuit model for each group of sequence components can be derived. The diagram for negative-sequence components is shown in Fig. 2, where the superscript “-” denotes negative sequence.

Figure shows the structure of a three-phase four-wire grid-interfacing system being connected to the utility grid at the PoC through LCL filters. It normally synchronizes with the utility grid and delivers electrical energy to the grid from the DC-bus when pre-regulated distributed sources are connected.

Similarly, the superscript “+” denotes positive sequence. Phasors V_g and V^-_s (in the following, complex numbers are denoted with a bar subscript) are the negative-sequence voltages of the utility grid and at the PoC, respectively. Current I^-_s is the negative-sequence current controlled by the grid-interfacing inverter. The equivalent line impedance is represented by Z_g , the equivalent impedance of the utility grid when the line impedances of the three phases are assumed symmetrical.

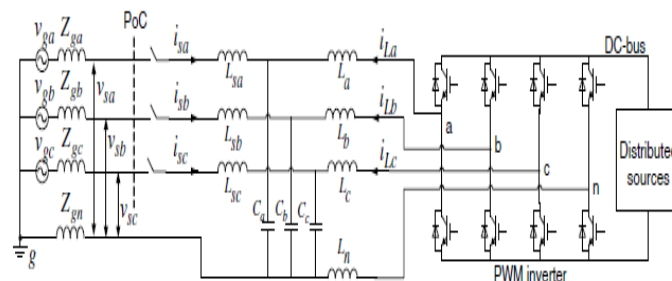


Fig:1(a): 3- ϕ four wire Grid interfacing inverter at PoC

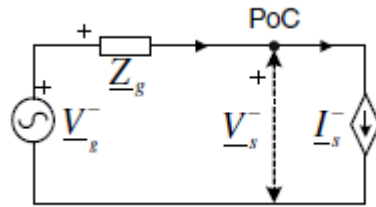


Fig 1(b): Negative sequence equivalent model

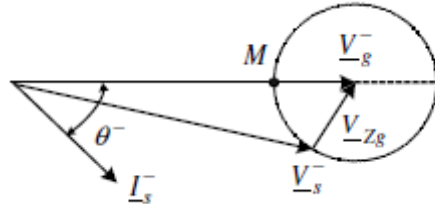


Fig 1(c):Phasor diagram of the Negative sequence model

Accordingly, a phasor diagram showing the change for negative-sequence fundamental current is drawn . By changing the amplitude and phase of the negative sequence current $I - s$, the negative-sequence voltage $V - s$ can be regulated through the voltage drops across the line impedance. For a given amplitude $I - s$, the voltage changes along the dashed circle and reaches a minimum value at the point M where $\theta -$ (the phase angle between negative sequence voltage and current) equals the negative of impedance angle of Z_g 's.

Similarly, zero-sequence voltages at the PoC can be compensated by regulating the zero-sequence currents within the system.

This paper only concentrates on the correction of negative-sequence voltages, considering zero-sequence voltages do not exist in case of three wire systems. Of course, zero-sequence voltages can be isolated by transformers when needed.

Furthermore, it is noted that measurements of zero-sequence components can be done simply by adding three-phase quantities, M while accurate positive- and negative-sequence components are difficult to be determined.

Therefore, zero sequence voltage correction can be trivially added to the control based on the proposed control scheme for negative-sequence voltage correction and is not discussed in this paper.

II. Control Scheme

2.1 DETERMINATION OF NEGATIVE-SEQUENCE CURRENTS

The basic principle of how to correct unbalanced voltage at the PoC with sequence-current control. It is suggested to determine the negative-sequence currents based on the voltage unbalance factor. To assess unbalanced voltages at the PoC, the voltage unbalance factor, KVUF is defined as the ratio between the amplitude of the negative-sequence voltage $V - s$ and the amplitude of the positive-sequence voltage $V + s$. The following constraint equation is proposed to calculate the desired current amplitude $I - s$:

$$\frac{I_s^-}{I_s^+} = \frac{V_s^-}{V_s^+} = K_{VUF}, \quad (1)$$

Where $I + s$ is the amplitude of the positive-sequence current. Then, the resulting $I - s$ is derived based on the ratio of unbalance voltages at the PoC from (1). However, the voltage unbalance factor at the PoC varies with the controlled negative-sequence currents, because the controller utilizes feed forward measurements of KVUF and operates in a open-loop. Consequently, this strategy may cause the value of KVUF in (1) to vary.

To ensure a stable correction, a smooth update method for KVUF is added to the control. The flow chart shown in Fig. 4 illustrates how to derive the final $I - s$. The currently measured quantity is referred to as $KVUF(n)$, and the previous one is $KVUF(n - 1)$. In Fig. 4, the minimum threshold (K_{min}) of negative-sequence correction is defined according to practical demands, and a coefficient denoted by λ is introduced for smooth regulation when decreasing the output value of KVUF. Note that, for system protection, the current rating of the inverters is always checked before returning $I - s$.

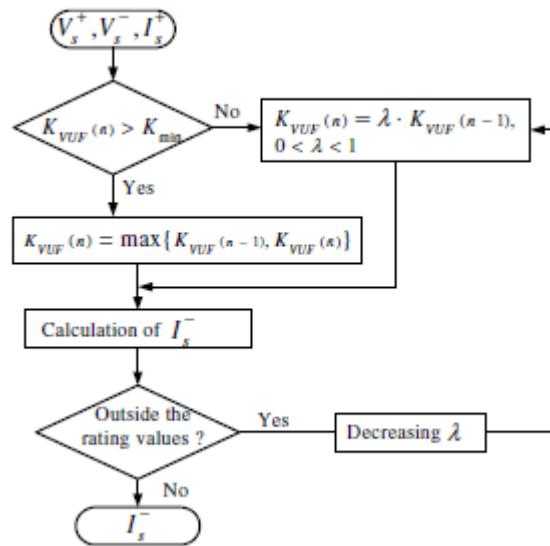


Fig 2.1: Flow chart of KVUF Determination

2.2. POSITIVE- AND NEGATIVE-SEQUENCE DETECTION

The factor KVUF is essential to get the amplitude of negative-sequence currents. Thus the separation of sequence voltages is central to get the value of KVUF, as well as to the synchronization with the utility grid. For unbalanced or distorted grid voltages, a multi-variable filter was introduced for detecting the positive-sequence component in the stationary frame. After modification, this filter is able to directly filter out the fundamental positive and negative-sequence vectors.

The following mathematically demonstrates the multi-variable filter for symmetric sequence decomposition. For unbalanced distorted voltages, the positive- and negative-sequence components are in the $\alpha - \beta$ frame

$$\begin{aligned} \underline{v}_{\alpha\beta}(t) &= v_{\alpha}(t) + jv_{\beta}(t) \\ &= \sum_{k=1}^{\infty} (\underline{V}_k^+ e^{jk\omega_1 t} + \underline{V}_k^{\circ} e^{-jk\omega_1 t}), \end{aligned} \quad (2)$$

as expressed by

where k denotes the harmonic number, ω_1 denotes the fundamental radian frequency, and the superscript symbol “o” denotes conjugate. Let us look for a filter $G^+(t)$, which can damp all harmonic components of $v_{\alpha\beta}(t)$ but the fundamental positive-sequence component in the stationary frame. That is,

$$\underline{v}_{\alpha\beta}(t) * \underline{G}^+(t) = \underline{v}'_{\alpha\beta}(t), \quad (3)$$

where the “*” denotes a convolution product, and

$$\begin{aligned} \underline{v}'_{\alpha\beta}(t) &= \underline{V}_1^+ e^{j\omega_1 t} + \sum_{k=3,5,\dots}^{\infty} \underline{U}_k^+ e^{jk\omega_1 t} \\ &\quad + \sum_{k=1,3,\dots}^{\infty} \underline{U}_k^{\circ} e^{-jk\omega_1 t} \end{aligned} \quad (4)$$

with $\|\underline{U}_k^+\| \ll \|\underline{V}_1^+\|$ and $\|\underline{U}_k^{\circ}\| \ll \|\underline{V}_1^-\|$.

$$\begin{aligned} \underline{v}_{\alpha\beta}(t)e^{-j\omega_1 t} &= \underline{V}_1^+ + \sum_{k=2,4,\dots}^{\infty} (\underline{V}_k^+ e^{jk\omega_1 t} + \underline{V}_k^{\circ} e^{-jk\omega_1 t}), \\ \underline{v}'_{\alpha\beta}(t)e^{-j\omega_1 t} &= \underline{V}_1^+ + \sum_{k=2,4,\dots}^{\infty} (\underline{U}_k^+ e^{jk\omega_1 t} + \underline{U}_k^{\circ} e^{-jk\omega_1 t}). \end{aligned} \quad (5)$$

$$L[\underline{H}(t)] = \underline{H}(s) = \frac{\omega_b}{s + \omega_b}, \quad (6)$$

$$(\underline{v}_{\alpha\beta}(t)e^{-j\omega_1 t}) * \underline{H}(t) = \underline{v}'_{\alpha\beta}(t)e^{-j\omega_1 t}, \quad (7)$$

$$\underline{v}_{\alpha\beta}(s + j\omega_1)\underline{H}(s) = \underline{v}'_{\alpha\beta}(s + j\omega_1). \quad (8)$$

$$\underline{v}_{\alpha\beta}(s) \cdot \frac{\omega_b}{s - j\omega_1 + \omega_b} = \underline{v}'_{\alpha\beta}(s). \quad (9)$$

$$\underline{v}_{\alpha\beta}(s)\underline{G}^+(s) = \underline{v}'_{\alpha\beta}(s). \quad (10)$$

$$\underline{G}^+(s) = \underline{H}(s - j\omega_1) = \frac{\omega_b}{s - j\omega_1 + \omega_b}. \quad (11)$$

By expanding (10) to

$$\underline{v}'_{\alpha}(s) + j\underline{v}'_{\beta}(s) = \frac{\omega_b}{s - j\omega_1 + \omega_b} [v_{\alpha}(s) + jv_{\beta}(s)], \quad (12)$$

the following equations are derived

$$\begin{aligned} \underline{v}'_{\alpha}(s) &= \frac{1}{s} [\omega_b(v_{\alpha}(s) - \underline{v}'_{\alpha}(s)) - \omega_1 \underline{v}'_{\beta}(s)], \\ \underline{v}'_{\beta}(s) &= \frac{1}{s} [\omega_b(v_{\beta}(s) - \underline{v}'_{\beta}(s)) + \omega_1 v_{\alpha}(s)]. \end{aligned} \quad (13)$$

Similarly, the fundamental negative-sequence component follows as

$$\underline{v}_{\alpha\beta}(t) * \underline{G}^-(t) = \underline{v}''_{\alpha\beta}(t), \quad (14)$$

where

$$\begin{aligned} \underline{v}''_{\alpha\beta}(t) &= \underline{V}_1^- e^{-j\omega_1 t} + \sum_{k=1,3,\dots}^{\infty} \underline{U}_k^+ e^{jk\omega_1 t} \\ &\quad + \sum_{k=3,5,\dots}^{\infty} \underline{U}_k^- e^{-jk\omega_1 t}, \end{aligned} \quad (15)$$

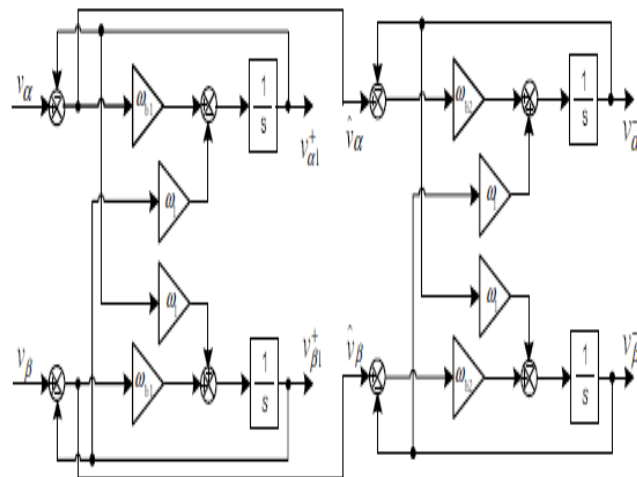


Fig 3: Implementation diagram of the multi variable filter

or $\underline{v}_{\alpha\beta}''(t) \approx \underline{v}_{\alpha\beta 1}^-(t)$. Similar to (8) and (10), we have

$$\begin{aligned} \underline{v}_{\alpha\beta}(s - j\omega_1) \cdot \underline{H}(s) &= \underline{v}_{\alpha\beta}''(s - j\omega_1), \\ \underline{v}_{\alpha\beta}(s) \cdot \underline{G}^-(s) &= \underline{v}_{\alpha\beta}''(s), \end{aligned} \quad (16)$$

where

$$\underline{G}^-(s) = \frac{\omega_b}{s + j\omega_1 + \omega_b}.$$

Correspondingly, the equations below are derived:

$$\begin{aligned} v_{\alpha}''(s) &= \frac{1}{s} [\omega_b(v_{\alpha}(s) - v_{\alpha}''(s)) + \omega_1 v_{\beta}''(s)], \\ v_{\beta}''(s) &= \frac{1}{s} [\omega_b(v_{\beta}(s) - v_{\beta}''(s)) - \omega_1 v_{\alpha}(s)]. \end{aligned} \quad (17)$$

Therefore, the detection for $v^+ \alpha 1(t) + jv^+ \beta 1(t)$ and $v^- \alpha 1(t) - jv^- \beta 1(t)$ are approximately achieved from (13) and (17). These equations can be easily implemented in the α - β frame by digital control, without complicated transformation to the SRF and the inverse transformation.

In practical applications, the negative-sequence component is too small to be detected accurately. This is because the input signals involve a large proportion of positive sequence components which are difficult to damp totally. Alternative signals $\underline{v}_{\alpha\beta}(t)$, with

$$\widehat{\underline{v}}_{\alpha\beta}(t) = \widehat{v}_{\alpha}(t) + j\widehat{v}_{\beta}(t) = \underline{v}_{\alpha\beta}(t) - \underline{v}_{\alpha\beta 1}^+(t), \quad (18)$$

where the dominant positive-sequence component $v^+ \alpha 1(t) + jv^+ \beta 1(t)$ is abstracted, and can be used as input signals. This will improve the filtering effect for negative-sequence quantities. Fig. 5 illustrates the implementation diagram of the multiple-variable filter, where the bandwidth ω_b for the positive- and negative-sequence filter is denoted by ω_{b1} and ω_{b2} respectively (the values can be different and adapted to practical situations). The central frequency ω_1 is set at the fundamental frequency of the grid voltage. In case of grid frequency variations the bandwidth can be increased slightly, or ω_1 can be adaptively updated with the measured fundamental frequency.

A frequency domain multi-variable filter plot is drawn based on (10) and the second equation in (16). Due to unity gain and zero phase-shift of the positive-sequence filter at the central frequency (50Hz), $v_{\alpha\beta}(t) + jv_{\beta}(t)$ can be directly derived. This manipulation is equivalent to a notch filter at the positive fundamental frequency, as shown in Figure

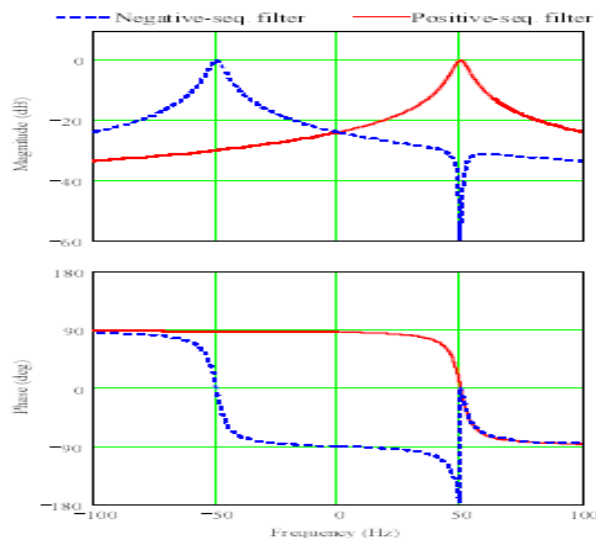


Fig 4:Multi variable filter plot in frequency domain with $\omega_1=314\text{rad/s}$; and $\omega_{b1}=\omega_{b2}=20$

III. Reference Signals Generation

Figure shows the block diagram of the inverter's current reference generator. It consists of the detection of symmetric sequence voltages with a multi-variable filter, the VUF calculation, average power regulation and the signal synthesis. The first two processes have been detailed in the previous two subsections.

By utilizing the fundamental positive- and negative-sequence components filtered out by the filter, we can obtain

$$\begin{aligned} V_{mag}^+ &= \sqrt{v_{\alpha 1}^+{}^2 + v_{\beta 1}^+{}^2}, \\ V_{mag}^- &= \sqrt{v_{\alpha 1}^-{}^2 + v_{\beta 1}^-{}^2}, \end{aligned} \quad (19)$$

Where V_{mag}^+ and V_{mag}^- denote the magnitude of fundamental positive- and negative-sequence voltage, respectively.

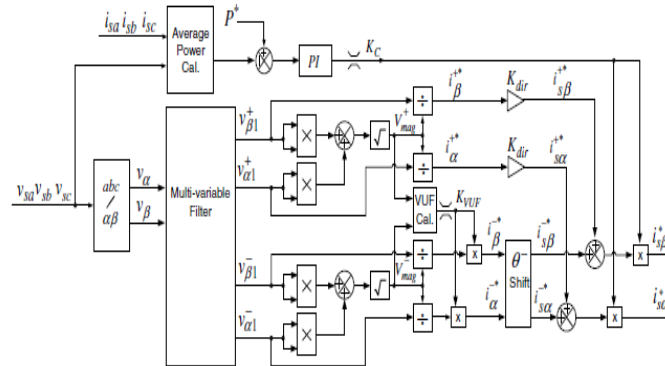


Fig 3.1: Current reference generation for the inverter control

Consequently, two groups of per-unit signals can be derived with divisions, that is $i^+_{\alpha} + j i^+_{\beta}$ and $i^-_{\alpha} + j i^-_{\beta}$. According to the principle described in section II, negative-sequence currents are designed to keep a phase-shift θ^- with the negative-sequence voltage. This phase-shift equals the negative line impedance angle for the maximum correction effect. Its mathematical derivation is

$$i^-_{s\alpha} + j i^-_{s\beta} = (i^-_{\alpha} + j i^-_{\beta}) e^{j\theta^-}. \quad (20)$$

The positive-sequence current references are either in phase or in anti-phase with the positive-sequence component of the grid voltage, depending on the desired direction for energy delivery. In this paper, the gain K_{dir} is set -1 in order to deliver energy to the utility grid.

In the average power control loop of figure the power reference P_{is} is given, which can be determined according to the application, such as the active power generated by upstream DG or the power demanded by the downstream utility grid.

In order to eliminate the effects of double fundamental frequency ripple on the measured average power, the parameters should have a small proportional gain and a big integration time constant. In this work, the gain is chosen as 0.04 and the time constant is 0.02s. The output of the PI controller is used to regulate the amplitudes of the desired currents with the coefficient K_c . All together, it follows that the current references $i^*_{s\alpha}$ and $i^*_{s\beta}$ are derived in the stationary frame. This is beneficial for the controller design, since the controller presented in the next section is also designed in the stationary frame. The mathematical manipulations to optimally implement the above digital process are not the subject of this paper, and will be discussed elsewhere.

IV. Controller for Current regulation

It is constructed by a double-loop current controller, that is an outer control loop with proportional-resonant (PR) controllers for eliminating the zero steady-state error of the delivered currents, and an inner capacitor current control loop with simple proportional controllers to improve stability. Figure shows the controller structure of the grid interfacing inverter

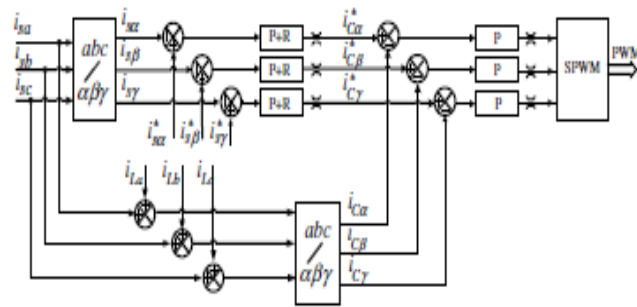


Fig 4.1: Structure of the controller for current regulation

$$G_i(s) = K_p + \frac{2K_r\omega_{br}s}{s^2 + 2\omega_{br}s + \omega_1^2}, \quad (21)$$

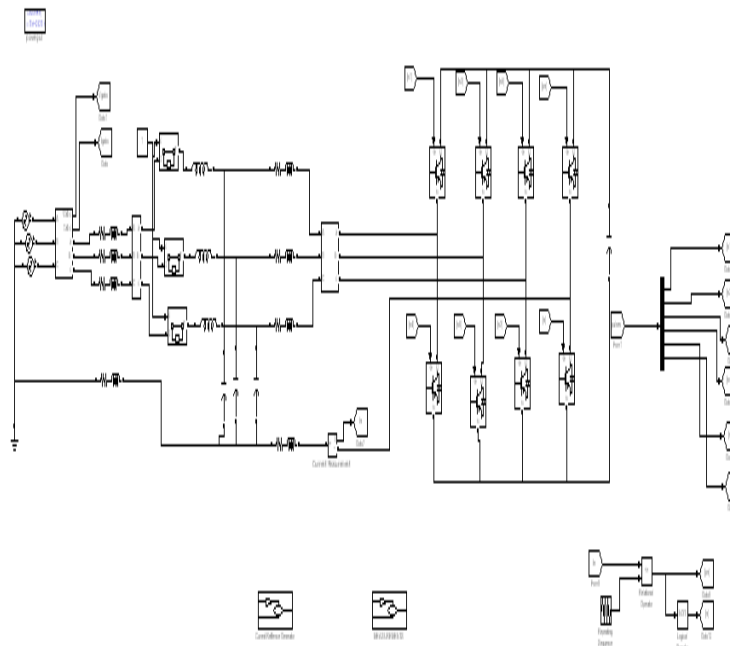
Instead of direct sampling, capacitor currents are calculated from the output currents and the inner filter inductor currents. These currents are measured anyway for over-current protection. To eliminate the zero-sequence currents in unbalanced situations, the current reference $i^*_{s\gamma}$ should be zero.

The control for both positive- and negative-sequence components would be much too complicated and computation-time consuming when conventional PI control with coordinate transformation were used.

Therefore, it is preferred to choose a PR controller in the stationary frame. A quasi-proportional-resonant controller with high gain at the fundamental frequency is used, where K_p is the proportional gain, K_r the resonant gain, and ω_{br} the equivalent bandwidth of the resonant controller. A detailed design for the PR controller has been presented in, it is not duplicated here. Through optimizing, the parameters used in the simulation and experiment are $K_p=0.5$, $K_r=50$, and $\omega_{br}=20$

V. Results:

Three-phase four wire grid-interfacing inverter at POC.



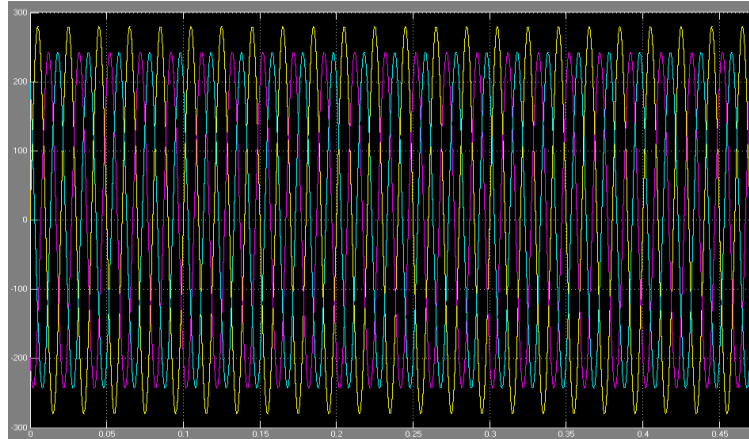


Fig (a): unbalanced grid voltages in a-b-c frame

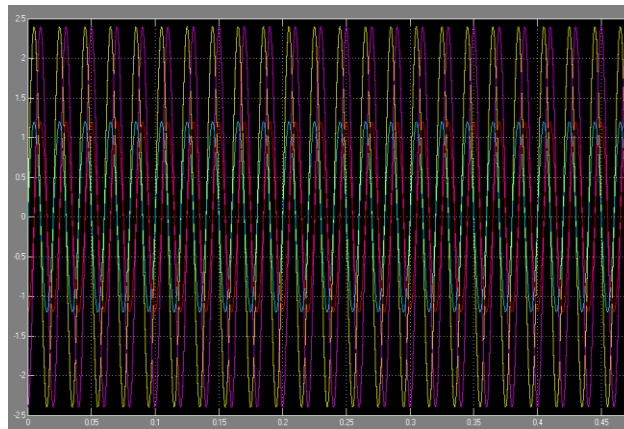


Fig (b): The per unit positive –sequence currents in phase with the positive sequence voltage

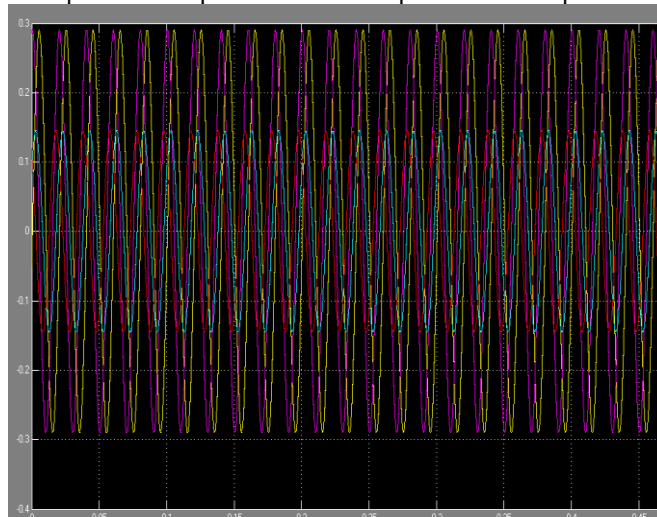


Fig (c): The negative sequence currents lags the negative sequence voltage by 45° in the α - β frames

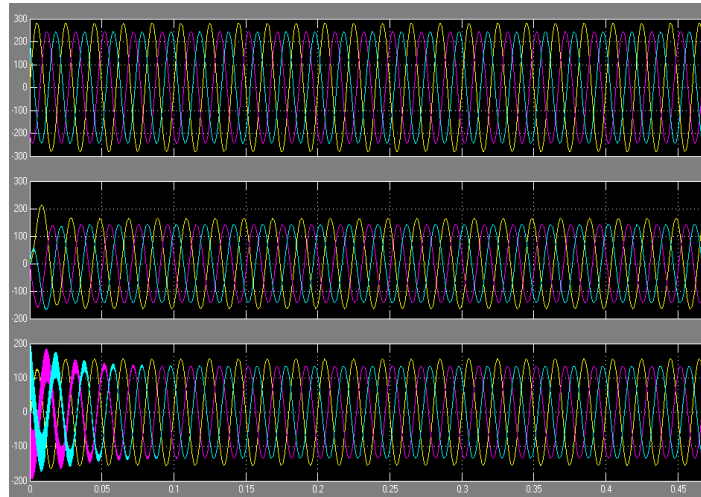


Fig (d): Experimental results of the grid-interfacing inverter with integrated voltage unbalance correction (a) unbalanced grid voltages,(b) currents delivered by the inverter, and (c) voltages at the PoC.

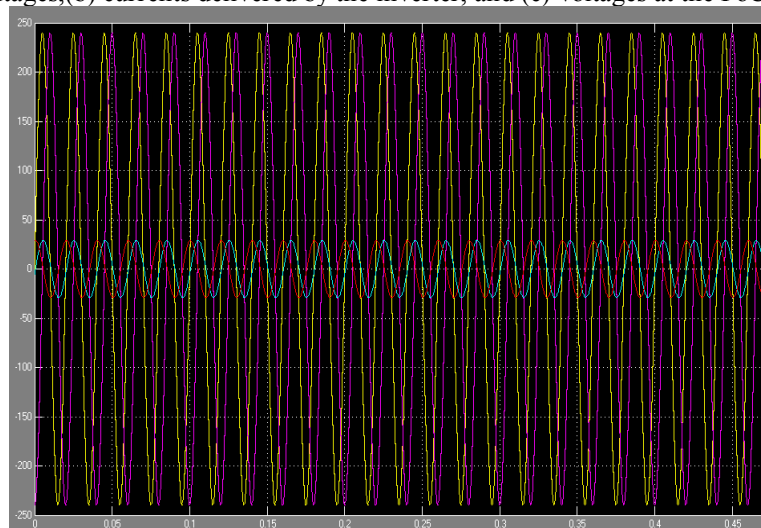


Fig (e):Experimental waveforms of positive- and negative-sequence voltage detection, where the filtered out fundamental symmetric sequence voltages are derived in the $\alpha - \beta$ frame.

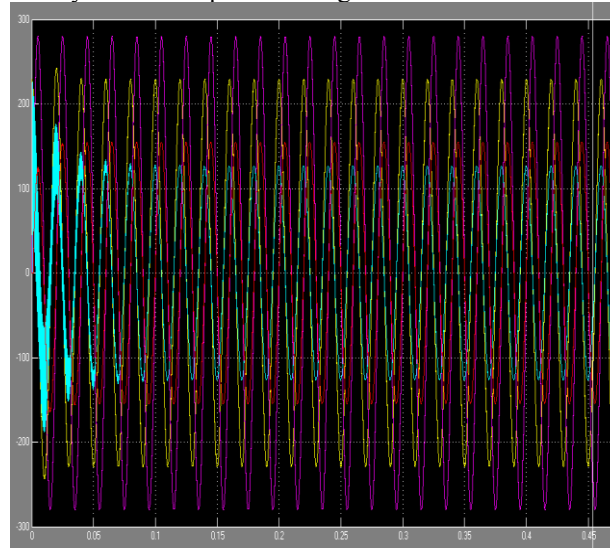


Fig (f): Experimental results of the negative-sequence voltage correction. The α, β components of the negative-sequence voltage of the PoC show a 10% amplitude reduction compared with the negative-sequence voltage of the grid

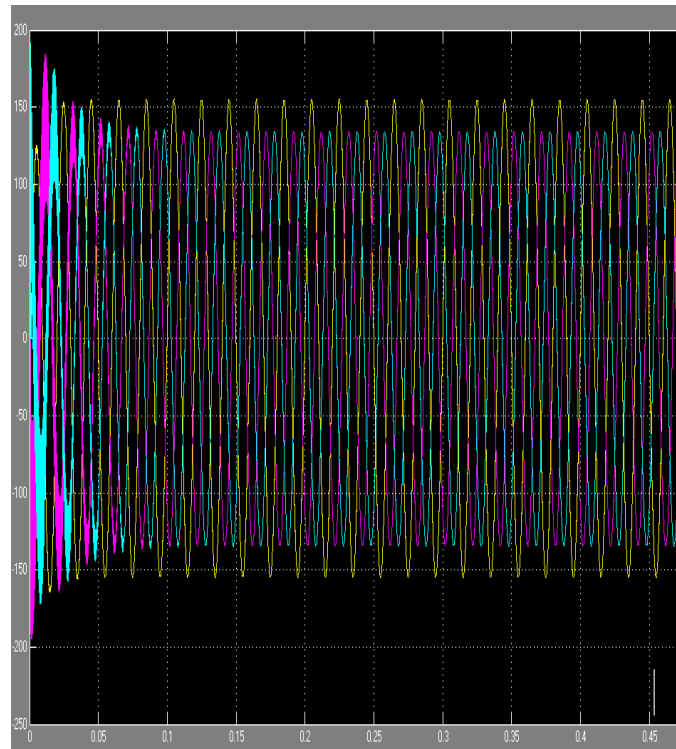


Fig (g):Experimental waveforms of the negative-sequence voltage correction. The resulting corrected voltages tend to be balanced.

References:

- [1] Annette von Jouanne and Basudeb (Ben) Banerjee, "Assessment of voltage unbalance," *IEEE Trans. Power Del.*, vol. 16, no. 4, pp. 782-790, Oct. 2001.
- [2] Hideaki Fujita, and H. Akagi, "Voltage-regulation performance of a shunt active filter intended for installation on a power distribution system," *IEEE Trans. Power Electron.*, vol 22, no. 3, pp. 1046-1053, May 2007.
- [3] Kuang Li, Jinjun Liu, and Zhaoan Wang, and Biao Wei, "Strategies and operating point optimization of STATCOM control for voltage unbalance mitigation in three-phase three-wire systems," *IEEE Trans. Power Del.*, vol. 22, no. 1, pp. 413-422, Jan. 2007.
- [4] Kalyan K. Sen, "SSSC-static synchronous series compensator theory, modeling, and application," *IEEE Trans. Power Del.*, vol. 13, no. 1, pp. 241-246, Jan. 1998.
- [5] Vijay B. Bhavaraju and Prasad N. Enjeti, "An active line conditioner to balance voltages in a three-phase system," *IEEE Trans. Ind. Applicat.*, vol. 32, no. 2, pp. 287-292, Mar./Apr. 1996.
- [6] Hideaki Fujita, H. Akagi, "The unified power quality conditioner: the integration of series- and shunt-active filters," *IEEE Trans. Power Electron.*, vol.13, no. 2, pp. 315-322, Mar. 1998.
- [7] Dusan Graovac, V. A. Katic, and A. Rufer, "Power quality problems compensation with universal power quality conditioning system," *IEEE Trans. Power Del.*, vol. 22, no. 2, pp. 968-976, Apr. 2007.
- [8] Koen J. P. Macken, Koen Vanthournout, Jeroen Van den Keybus, Geert Deconinck, and Ronnie J. M. Belmans, "Distributed Control of Renewable Generation Units With Integrated Active Filter," *IEEE Trans. Power Electron.*, vol. 19, no. 5, pp. 1353-1360, Sep. 2004.

A.MOHAN: Studying M-Tech in power electronics at



Sri Venkateshwara Engineering College ,Suryapet his interested in Power Electronics, Power Systems and non conventional energy systems



D.NAGARAJU: Working as a Sr. Assistant Professor at

Sri Venkateshwara Engineering College ,Suryapet his interested in Power Electronics, Power Systems and non conventional energy systems